Manuscript prepared for Atmos. Chem. Phys. Discuss.
with version 2015/04/24 7.83 Copernicus papers of the LaTeX class copernicus.cls.
Date: 6 April 2016

First continuous ground-based observations of long period oscillations in the vertically resolved wind field of the stratosphere and mesosphere

R. Rüfenacht, K. Hocke, and N. Kämpfer

Institute of Applied Physics, University of Bern, Bern, Switzerland

Correspondence to: R. Rüfenacht (rolf.ruefenacht@iap.unibe.ch)

Abstract

Direct measurements of middle-atmospheric wind oscillations with periods between 5 and 50 days in the altitude range between mid-stratosphere (5 hPa) and upper mesosphere (0.02 hPa) have been made using a novel ground-based Doppler wind radiometer. The oscillations were not inferred from tracer measurements, as the radiometer offers the unique capability of near-continuous horizontal wind profile measurements. Observations from four campaigns at high, mid and low latitudes with an average duration of 10 months have been analyzed. The dominant oscillation has mostly been found to lie in the extra-long period range (20–50 days), while the well-known atmospheric normal modes around 5, 10 and 16 days have also been observed. Comparisons of our results with ECMWF Operational Analysis data revealed remarkably good agreement below 0.3 hPa but discrepancies above.

1 Introduction

The dynamics of the middle atmosphere is characterized by waves and oscillations with distinct periods. An accurate representation of the middle-atmospheric dynamics can improve the forecast skills of numerical weather prediction models, especially on time scales beyond one week (e.g. Baldwin et al., 2003b, a; Charlton et al., 2004; Hardiman et al., 2011; Sigmond et al., 2013). Therefore validation of these models is needed also in the stratosphere and mesosphere in addition to tropospheric analyses. Thereby not only the correctness of the absolute values of the atmospheric parameters, but also the correct representation of their natural oscillations should be studied as such oscillations play an important role in the dynamics of the middle atmosphere.

Measurements of zonal and meridional wind are the most direct way to observe atmospheric dynamics. For studying long period oscillations long time series of continuous measurements are required. However, wind observations in the upper stratosphere and

lower mesosphere are practically non-existent and the few measurements available are not present on a continuous basis (see Supplement Text S1).

Rocket soundings (e.g. National Research Council, 1966; Müllemann and Lübken, 2005) and the Doppler wind lidar at ALOMAR (Hildebrand et al., 2012; Baumgarten, 2010) have been used to retrieve vertical profiles of horizontal wind throughout the stratosphere and mesosphere. However the novel ground-based microwave wind radiometer WIRA (Rüfenacht et al., 2012, 2014) is the only instrument capable of providing wind observations between 35 and 70 km altitude (5 to 0.04 hPa) with time series satisfying the requirement of long term continuity. Presently, the published wind lidar data sets are too short for long period spectral analyses. The coarse time resolution of rocket soundings seems inadequate for the investigation of oscillations with periods shorter than approximatively 20 days. A rocket-sensed wind data set with 1–2 profiles per week has, however, been used by Keckhut (1995) in a study investigating the effect of the 27-day solar rotation period on middle atmospheric dynamics.

Oscillations of horizontal wind in the (upper) mesosphere/lower thermosphere (MLT) have been extensively studied using radar observations (e.g. Araújo et al., 2014; Day et al., 2012; Guharay et al., 2014; Luo et al., 2001, 2002). In the upper stratosphere and lower mesosphere region analyses of long period oscillations in the concentration of trace gases, such as ozone and water vapor, have been reported based on microwave radiometry (e.g. Hocke et al., 2013; Scheiben et al., 2014).

Here we present an analysis of oscillations in upper stratospheric and mesospheric horizontal wind profiles with periods between 5 and 50 days. We also compare results obtained from wind radiometer measurements to the Operational Analysis data from the European Centre for Medium-Range Weather Forecast model (ECMWF).

2 Data sets

2.1 Wind radiometer data

The Doppler WInd RAdiometer WIRA is a novel ground-based passive heterodyne receiver designed for the observation of horizontal wind profiles from the mid-stratosphere (5 hPa) to the mesopause (0.02 hPa) where no other application provides continuous time series of wind measurements. Wind profiles are determined by measuring Doppler shifts of the pressure broadened emission line of ozone at 142 GHz. The retrieval from the raw data is based on an optimal estimation inversion (Rodgers, 2000) of an atmospheric radiative transfer model implemented in the ARTS/QPACK software (Eriksson et al., 2011, 2005). Typical measurement uncertainties and vertical resolutions of the daily average wind profiles used in this study range from 10 to 20 $\mathrm{m\,s^{-1}}$ and from 10 to 16 km, respectively. However, as indicated by Rodgers (2000), features vertically spaced by less than 10 km can in many cases be recognized as individual peaks in the retrieved data, although their amplitudes are not independent. Detailed descriptions of the instrument and retrieval characteristics of WIRA have already been published (Rüfenacht et al., 2012, 2014).

A strength of microwave radiometers is their ability to take measurements during day and night and under overcast conditions. This strength, combined with low operation costs, allows for the recording of long continuous time series. The present study is based on measurements taken by WIRA at four different locations at high, mid and low latitudes: Sodankylä (67°22′ N/26°38′ E, October 2011–July 2012), Bern (46°57′ N/7°26′ E, September 2010–July 2011), Observatoire de Haute-Provence (43°56′ N/5°43′ E, November 2012–May 2013) and Observatoire du Maïdo on La Réunion (21°04′ S/55°23′ E, September 2013–February 2015). The data series from these campaigns are plotted in Fig. 1. At Sodankylä and Bern only zonal wind was measured, whereas the observations from Provence and La Réunion comprise both zonal and meridional components. The gray areas in Fig. 1 correspond to data points judged untrustworthy (measurement response < 0.8, altitude resolution > 20 km or altitude accuracy > 4 km, see Rüfenacht et al., 2014, for details). The sensitive altitude range largely depends on the signal-to-noise ratio of the re-

ceiver, which was significantly improved by an instrumental upgrade in autumn 2012. Moreover the strength of the radiation signal reaching the receiver depends on tropospheric conditions. While ice clouds are fully transparent to microwave radiation near 142 GHz, attenuation by liquid and gaseous water can negatively impact the signal-to-noise ratio, although observations remain possible even in the presence of non-precipitating liquid water clouds or fog.

2.2 ECMWF model data

The European Centre for Medium-Range Weather Forecasts (ECMWF) is a major service provider of weather and climate data products. The Operational Analysis used in this study combines meteorological data from a variety of different observing platforms with a continually updated general circulation model. The observations assimilated in a 4-D-Var assimilations window of 12 h mainly originate from the troposphere and lower stratosphere (e.g. Dee et al., 2011; ECMWF, 2016). The few observations assimilated at higher altitudes mainly originate from infrared radiation soundings (Engelen and Bauer, 2014; Dragani and McNally, 2013, and references therein). Operational Analysis is preferred over the reanalysis, i.e. ERA-Interim, principally because of the higher model top (0.01 hPa compared to 0.1 hPa). For the research presented here data from model versions 36r2 (September to November 2010), 36r4 (November 2010 to May 2011), 37r2 (May to November 2011), 37r3 (November 2011 to June 2012), 38r1 (June 2012 to June 2013), 38r2 (June to November 2013) and 40r1 (November 2013 to February 2015) with a spectral resolution of T1279 have been used (ECMWF, 2015). The analog of Fig. 1 for the ECMWF data used in the present study is given in Fig. S2 of the Supplement. A previous study revealed agreement within the measurement error between ECMWF's Operational Analysis and WIRA's wind measurements in the stratosphere, but demonstrated that the mesospheric zonal wind speed is generally significantly larger in the model for mid and high latitude stations (Rüfenacht et al., 2014). In contrast, comparisons between a limited data set of WIRA and the MERRA re-analysis from NASA's GEOS-5 model (Rienecker et al., 2011) revealed good agreement also in the mesosphere (Le Pichon et al., 2015).

3 Data analysis

It is known from earlier research that atmospheric waves with periods ranging from 5–50 days are intermittent, showing little phase preference (e.g. Araújo et al., 2014; Day et al., 2012). Therefore we perform the spectral analyses in sliding Hamming windows encompassing three oscillation periods T. The window width matching an integer multiple of the searched period and the use of a Hamming windowing function help to minimize spectral leakage. Data gaps in the measured time series can be large at some times and altitudes, therefore gaps were not interpolated as done in other studies, because this would artificially alter the oscillation signal (damping it in case of linear interpolation). They were rather treated as missing values and the Lomb–Scargle spectral approach for irregularly spaced data was applied (Press et al., 2001; Scargle, 1982; Lomb, 1976).

The spectral method used in the present study will be described in some more details in the following: For each altitude level a wind time series $\boldsymbol{x}$ is sampled at equally spaced times $t_j = k \cdot \delta t$ with $x_j = \boldsymbol{x}(t_j)$ and $k \in \mathbb{N}$. However, for some t_j no reliable measurement data x_j exist at the respective altitude. Such pairs of (t_j, x_j) will be excluded from the following analysis leading to an unequally spaced time series. We define $\bar{x}_j$ and σ_j as the mean and standard deviation of $\boldsymbol{x}$ in the index range $(j-n)\ldots(j+n)$, i.e. within a window of length $(2n+1) \approx 3T/\delta t$. The Lomb–Scargle transform $\mathcal{L}$ is applied to the windowed time series to obtain a normalized periodogram P_j for each point in time:

$$P_j = \mathcal{L}_{i \in \mathcal{B}_j} \{ t_{j+i}, h_i \cdot (x_{j+i} - \bar{x}_j) \} \tag{1}$$

with the indices i in the range

$$\mathcal{B}_j = \{ m \,|\, m \in \{-n, -n+1, \ldots, 0, \ldots, n\} \wedge \exists x_{j+m} \} \tag{2}$$

and with h_i being the coefficient of a Hamming window of length $(2n+1)$ centered around index 0. Let us also define:

$$\mathcal{C}_j = \{ m \,|\, m \in \mathcal{B}_j \wedge |m| \cdot \delta t \leq T/2 \}, \tag{3}$$

i.e. $\mathcal{C}_j$ denotes the central third of $\mathcal{B}_j$. P_j's calculated from windows with an insufficient amount of relevant data points, i.e. when

$$\#\mathcal{B}_j < \frac{T}{\delta t} \quad \vee \quad \#\mathcal{C}_j < \frac{T}{3\delta t} \tag{4}$$

are rejected from the analysis. The entire procedure is repeated for all searched oscillation periods T, for all times t_j and for all altitude levels. In Eqs. (2) to (4) $\wedge$ and $\vee$ denote logical "and" and "or" while the cardinality operator $\#$ returns the number of elements of its argument.

The normalized periodogram P_j is readily transformed to the amplitude spectrum (e.g. by combining Eq. 6 from Hocke, 1998, and Eq. 15 from Harris, 1978):

$$A_j(T) = 2\sigma_j \sqrt{\frac{\sum_{i\in\mathcal{B}_j} h_i^2}{\left(\sum_{i\in\mathcal{B}_j} h_i\right)^2} P_j(T)}\,. \tag{5}$$

P_j also contains the information about the significance α of an oscillation peak at a distinct frequency

$$\alpha_j(T) = 1 - [1 - \exp(-P_j(T))]^M\,. \tag{6}$$

In our case M is a factor close to the window width (for details see Press et al., 2001). The variable α might also be referred to as "false alarm probability of the detection", a small α value indicates a highly significant oscillation.

For comparison, the pseudo-wavelet approach used by Studer et al. (2012) and Scheiben et al. (2014) has been modified in order not to rely on interpolation. The difference between the results obtained with the modified pseudo-wavelet method shown in Figs. S3 and S4 in the Supplement and the outcomes of the Lomb–Scargle method (Figs. 2 and 5) was found to be small. Moreover, the different spectral methods with and without interpolation and with different windowing functions have been tested for their ability of retrieving synthetic

oscillation signals containing data gaps correctly. The Lomb–Scargle method used with a Hamming window applied in the analyses presented in this paper was most successful and produced only marginal differences between the retrieved and the initial signal, but the pseudo-wavelet approach without interpolation of the data gaps used for Figs. S3 and S4 also provided satisfying results.

4 Results

Spectral analyses have been performed on daily average wind profiles by WIRA and ECMWF Operational Analysis. In order to allow direct comparisons between measurements and model, the ECMWF data were convolved with WIRA's averaging kernels to account for the limited vertical resolution of the radiometer and data gaps were added at the times t_j where the measurement did not provide reliable data. In the following, the model data treated in this way are referred to as "ECMWF at WIRA".

4.1 Altitude dependence of the periodograms

The altitude dependent temporally averaged periodograms of the horizontal wind measurements by WIRA are shown in Fig. 2. The temporal average runs over all oscillation amplitude data existing at a certain altitude for the respective campaign. From Fig. 1 one can identify levels where trustworthy measurement data are predominantly present during winter, because the generally wetter summer troposphere alters the signal-to-noise ratio of the observation setup as a consequence of a stronger attenuation of the middle-atmospheric radiation. At these altitudes the oscillation amplitudes should thus not be interpreted as averages over the entire duration of the campaign. This is especially the case for the upper altitude data from Sodankylä (above approx. 0.2 hPa) but to a lesser extent also applies to the other stations.

Figure 2 indicates that the dominant oscillations in horizontal wind occur in the extra-long period range (20–50 days) at all stations. Atmospheric oscillations with periods around 27 days are often discussed in the context of the modulation of the solar forcing with the

rotational period of the sun (e.g. Fedulina et al., 2004; Huang et al., 2015). However, cross-correlation analyses of WIRA's wind measurements with solar UV irradiance data revealed that the phase difference between wind and irradiance time series varies significantly for the different measurement campaigns. From this fact and from the obvious seasonality (see Sect. 4.2) of these wind oscillations observed during the maximum phase of solar cycle 24 we infer that the influences of the variations in the solar forcing on middle atmospheric horizontal winds must be indirect, if existing. Similar conclusions were drawn by a study with the WACCM model to be presented in a separate publication where it is demonstrated that periods around 27 days can also be produced inherently by the atmosphere and that oscillations in the solar irradiance can manifest themselves in the atmospheric wind periodograms at frequencies differing from the variations in solar forcing (Ansgar Schanz, personal communication, 2015). Huang et al. (2015) indicate that their observed extra-long period oscillation might be an atmospheric normal mode and that it may be indirectly introduced by the modulation of tropospheric convective activity with the solar rotation period. Fedulina et al. (2004) report a modulation of the 5-day wave amplitude with a period of 25 to 35 days but point out that a correlation with solar activity might appear by coincidence regarding the considered time scales.

Normal modes in the atmosphere are known to have oscillation periods around 2, 5, 10 and 16 days (Salby, 1981a, b) which can also be observed in the average periodograms of WIRA measurements for the different campaigns. According to the Nyquist theorem, measurements of daily average wind profiles do not allow to draw meaningful conclusions regarding the behavior of the quasi 2-day periodicity. A quasi 5-day wave is observed in WIRA's zonal wind measurements for Bern and Sodankylä, and for the zonal and meridional winds on La Réunion. The 5-day signal in the meridional wind in Provence has lower significance and seems to be an artifact of the measurement situation as it is also present in Fig. 3 showing "ECMWF at WIRA" data but not in the periodogram of the unaltered ECMWF data in Fig. 4. It might originate from the small data gap at the beginning of January 2013 (see Figs. 5 and 6) at a time of high variability due to a major sudden stratospheric warming. Oscillations with periods around 10 days are clearly visible in the zonal wind in So-

dankylä and the zonal and meridional wind in Provence. A quasi 16-day variation is weakly recognizable in the zonal wind measurements from La Réunion.

High interannual variability has to be expected (e.g. compare the results from the Bern and the Provence campaign which were sampled at very close geographical locations). Despite this variability, one might conclude from the WIRA data that zonal wind oscillations tend to be strongest at mid latitudes, and that meridional wind oscillations are weaker in the tropics than at mid-latitudes. This hypothesis is supported by Figs. S5 to S8 showing ECMWF data for more extended time intervals at the campaign sites. It also confirms previous studies based on observations or assimilated model data (Hirota and Hirooka, 1984; Hirooka and Hirota, 1985; Day et al., 2011; Fedulina et al., 2004). The highest oscillation amplitudes are usually detected around the stratopause which is also the region where the highest absolute wind speeds are generally observed (e.g. Rüfenacht et al., 2014). The reduced wave activity in the mesosphere, particularly above 0.1 hPa, may be explained by planetary wave breaking in the stratosphere (e.g. McIntyre and Palmer, 1983; Brasseur and Solomon, 2005). Interestingly this consideration also applies to the extra-long period oscillations what is in line with the periodograms of geopotential heights from MLS at mid-latitudes presented by Studer et al. (2012). In the interpretation of Fig. 2 we should keep in mind that the limited vertical resolution of WIRA, which is around 12 km (i.e. 0.75 pressure decades) at these altitudes, may vertically smear out the oscillation peaks.

The only major exception to the quiet mesosphere in Fig. 2 is the 27-day peak around 0.1 hPa in the periodogram for Sodankylä. This oscillation can probably be regarded as a special case as it occurs in the vicinity of the major sudden stratospheric warming event of January 2012 as seen from supplementary Fig. S13 which displays the oscillation activity at 0.05 hPa. Although based on very few data points, the slight increase near the 16-day periodicity at the very top of the retrieval range might be understood as an influence of the strengthening of this signal in the MLT region reported by other observational studies (e.g. Williams and Avery, 1992; Day et al., 2012).

The analysis for the scenario ECMWF at WIRA shown in Fig. 3 should yield identical results as presented in Fig. 2 if the measurements are error-free and the atmosphere is

realistically represented by the model. In this case WIRA and ECMWF would agree that the periodograms of the real atmosphere correspond to Fig. 4. The qualitative and quantitative agreement between measurements and model is remarkably good below 0.3 hPa. The only notable discrepancies occur at periods larger than 45 days, for the 5-day wave which is mostly absent in ECMWF and for the 10-day periodicity. The last one is present in ECMWF with amplitudes comparable to WIRA only for the meridional wind during the Provence campaign.

Above 0.3 hPa ECMWF tends to produce higher oscillation amplitudes than WIRA. Wind oscillation amplitudes observed in the MLT region (e.g. Araújo et al., 2014; Luo et al., 2001, 2002) better match with the uppermost observations from WIRA than with the high amplitudes in the ECMWF model.

A previous study (Rüfenacht et al., 2014) has shown that, in comparison with WIRA, ECMWF generally features stronger mesospheric zonal winds with discrepancies increasing for higher altitudes. When normalizing the oscillation amplitudes by dividing by the mean wind profile of the measurement campaign at the respective altitude the differences between WIRA and ECMWF were highly diminished (Fig. S13 in the Supplement). This shows that the oscillation amplitude discrepancy behaves similarly to the absolute wind speed discrepancy, i.e. increases by the same factor with increasing altitude. Knowing that the ECMWF model is constrained by the assimilation of tropospheric and stratospheric data but is mainly free-running in the mesosphere (Orr et al., 2010; ECMWF, 2016), one might conclude that some of ECMWF's model physics are not accurate enough to reproduce the dynamics of the mesosphere in detail. An overestimation of the upward transport of horizontal momentum or an underestimation of some damping mechanisms in the mesosphere are possible causes of this effect. Another explanation might be that the model contains assumptions on the balance between the wind and temperature fields which are not accurate in the mesosphere. As noted by Shepherd et al. (2000) and Koshyk et al. (1999) the unbalanced component of the flow increases with altitude. However, the exact reason for the concomitant mesospheric discrepancies between ECMWF's and WIRA's absolute wind speeds and oscillation amplitudes remain unclear.

4.2 Temporal evolution of the periodograms

Atmospheric waves and oscillations can be intermittent in nature (i.e. wave-packets) and/or seasonally constrained. Accordingly, the temporal evolution of the oscillations was examined. Figures 5, 6 and 7 display the results for WIRA, ECMWF at WIRA and unaltered ECMWF data, respectively, at stratopause level where the highest amplitudes have generally been observed. Contours indicating the significance levels of the oscillation peaks according to Eq. (6) are overlaid to the amplitude plots. Again, Fig. 7 would show the behavior of the real atmosphere represented by the measurements of WIRA in case Figs. 5 and 6 exactly match.

From the analyses it becomes obvious that the dominant oscillation in the extra-long period range is always highly significant. The oscillation peaks for ECMWF data are slightly more significant what is consistent with the absence of measurement noise.

A clear seasonality is apparent for all observations and model data with oscillation activities being much stronger in the winter half year for all oscillation periods covered by the present study. The seasonality is also visible for other years at the campaign sites as shown by ECMWF data (Figs. S9 to S12 of the Supplement) and is in accordance with other observational studies of stratopause level oscillations (Hirooka and Hirota, 1985; Day et al., 2011; Studer et al., 2012) and especially with the climatological periodogram of zonal wind at 58 km in Fig. 5 of Luo et al. (2001). As in the mentioned climatology, no quasi 5-day wave signature could be found in the summer data from WIRA, in contrast to the results of Hirota and Hirooka (1984) and Fedulina et al. (2004) which indicate the frequent presence of such a wave at the summer stratopause.

The same pattern of seasonality as for the high and mid latitude stations is observed on La Réunion although it is located in the southern tropics (21°04′ S). One can infer that the station is substantially influenced by mid-latitude dynamics. This influence is also recognizable in the time series of the observed zonal wind (Fig. 1) where the mid-latitudinal annual variation mostly dominates over tropical semi-annual variation, although the latter one is still clearly visible.

During WIRA's measurement campaigns in the Northern Hemisphere two major sudden stratospheric warmings occurred in mid January 2012 and at the beginning of January 2013. Previous studies (e.g. Alexander and Shepherd, 2010; Day et al., 2011; Scheiben et al., 2014) reported a strong decrease in planetary wave activity in the days and weeks following the onset of major warmings. This feature can nicely be seen in WIRA and ECMWF data for the Provence campaign, but the effect is absent from both data sets for the Sodankylä campaign.

The period of the extra-long period oscillations is not constant between the different campaigns. It can even vary within a single occurrence of the oscillation as seen in the example of Bern where the period decreases from 35 to 25 days between December 2010 and March 2011. A 10 days period change is at the limit of the spectral resolution of our analysis method for this long periodicities. Nevertheless it may be interpreted as a real signal, not only due to the monotony of the decrease, but also to an additional check using our spectral method with rectangular instead of Hamming windowing in order to improve the spectral resolution (not shown). A similar feature has simultaneously been observed at three different sites from high to lower mid-latitudes in the mesopause region by Luo et al. (2001). This study also noted that the extra-long period oscillation often appears in combination with a quasi 16-day wave. The occurrence of this periodicity has not been obvious from Figs. 2 and 3 because it had been masked by other oscillation signals in the temporal average. In contrast, it is clearly identifiable as independent periodicity in Figs. 5 and 6. In the Bern and the La Réunion time series the strongest 16-day amplitudes (lasting for about 1 period) are observed near the initiation and the termination of the persistent extra-long period oscillation with a duration of 80 and 50 days, respectively. The duration of the presence of these oscillations is comparable to the results for mesopause wind presented by Luo et al. (2001). However, it should be noted that if the extra-long period oscillation is abruptly initiated or terminated, the 16-day signal could be produced as an artifact of the used spectral method as simulations showed. Whether a real 16-day wave is present and whether the two oscillations are linked in some way will have to be verified in further studies.

In general the agreement between WIRA and ECMWF at stratopause level is very good in terms of timing, amplitude and frequency. The extra-long oscillations in zonal wind at the two mid latitude stations of Bern and Provence are slightly stronger in the WIRA time series and the amplitude of the quasi 16-day wave in the zonal wind is slightly enhanced for the measurements. However, the most notable difference between WIRA and ECMWF appears at shorter periods. Although mostly not statistically significant, ECMWF seems to underestimate variablities with periods shorter than 10 days for all measurement campaigns. A similar feature has been found for the comparison of middle-atmospheric temperature lidar observations from Observatoire de Haute Provence and Table Mountain (34°24′ N, 117°42′ W) with ECMWF model data (Le Pichon et al., 2015).

5 Conclusions

Long and extra-long period oscillations in the horizontal wind have been observed by the novel ground-based Doppler wind radiometer WIRA in the altitude range between mid-stratosphere (5 hPa) and upper mesosphere (0.02 hPa) at low, mid and high latitudes. In this altitude range wind observations are extremely sparse and the measurement time series from WIRA are the only ones satisfying the necessary conditions for the study of this type of oscillations.

The dominant oscillations were found to lie in the extra-long period band (20–50 days) with the features showing pronounced temporal intermittency and the period being subject to temporal variations. A direct link between the solar forcing and these atmospheric periodicities could not be established, however solar forcing might influence the atmospheric wave pattern in an indirect way. Enhanced quasi 16-day oscillation activity has sometimes been detected in the vicinity of strong extra-long period oscillations. A more extended study would however be needed to establish the origin of this signal and to uncover a potential link between the quasi 16-day wave and the extra-long periodicities. In addition to the extra-long period oscillations, normal modes with periods near 5, 10 and 16 days are present in our observations. All observed oscillations manifest a strong seasonality with amplitudes being

much higher during the winter half year. The strongest oscillation amplitudes were usually found around the stratopause.

WIRA observations and ECMWF model data agree remarkably well below 0.3 hPa. At higher altitudes ECMWF features higher oscillation amplitudes than the observations, a discrepancy behaving similarly to what has been noted for the discrepancy in absolute wind speeds in a previous study. In addition, ECMWF Operational Analysis data shows reduced variability at periods below 10 days as compared with the measurements by WIRA. More detailed validations of numerical weather prediction models such as ECMWF in the middle-atmosphere will be an important task for the near future and shall among others be addressed in the framework of the ARISE project (Blanc et al., 2015). Wind radiometer data could provide a valuable contribution to such research.

Data availability

We acknowledge ECMWF for the Operational Analysis data (www.ecmwf.int) as well as NASA for the Aura MLS temperature profiles (http://disc.gsfc.nasa.gov/acdisc) used in WIRA's retrieval algorithm in the way described in Rüfenacht et al. (2014). The WIRA data presented in this manuscript can be made available on request.

The Supplement related to this article is available online at doi:10.5194/acpd-0-1-2016-supplement.

Acknowledgements. This work has been supported by the Swiss National Science Foundation grants number 200020–146388 and 200020–160048. We especially thank the staff of the Observatoire du Maïdo, of the Observatoire de Haute-Provence and of the Finnish Meteorological Institute in Sodankylä for the hospitality and support during the measurement campaigns.

References

Alexander, S. P. and Shepherd, M. G.: Planetary wave activity in the polar lower stratosphere, Atmos. Chem. Phys., 10, 707–718, doi:10.5194/acp-10-707-2010, 2010.

Allan, D.: Statistics of atomic frequency standards, P. IEEE, 54, 221–230, doi:10.1109/PROC.1966.4634, 1966.

Araújo, L. R., Lima, L. M., Batista, P. P., Clemesha, B. R., and Takahashi, H.: Planetary wave seasonality from meteor wind measurements at 7.4° S and 22.7° S, Ann. Geophys., 32, 519–531, doi:10.5194/angeo-32-519-2014, 2014.

Baldwin, M. P., Stephenson, D. B., Thompson, D. W. J., Dunkerton, T. J., Charlton, A. J., and O'Neill, A.: Stratospheric memory and skill of extended-range weather forecasts, Science, 301, 636–640, doi:10.1126/science.1087143, 2003a.

Baldwin, M. P., Thompson, D. W. J., Shuckburgh, E. F., Norton, W. A., and Gillett, N. P.: Weather from the stratosphere?, Science, 301, 317–319, doi:10.1126/science.1085688, 2003b.

Baumgarten, G.: Doppler Rayleigh/Mie/Raman lidar for wind and temperature measurements in the middle atmosphere up to 80 km, Atmos. Meas. Tech., 3, 1509–1518, doi:10.5194/amt-3-1509-2010, 2010.

Blanc, E., Charlton-Perez, A., Keckhut, P., Evers, L., Heinrich, P., Le Pichon, A., and Hauchecorne, A.: The ARISE project: dynamics of the atmosphere and climat, Our Common Future Under Climate Change, International Scientific Coference, https://hal-insu.archives-ouvertes.fr/insu-01183228, poster, 2015.

Brasseur, B. H. and Solomon, S.: Aeronomy of the Middle Atmosphere, Springer, 3rd edn., 2005.

Charlton, A. J., O'Neill, A., Lahoz, W. A., and Massacand, A. C.: Sensitivity of tropospheric forecasts to stratospheric initial conditions, Q. J. Roy. Meteor. Soc., 130, 1771–1792, doi:10.1256/qj.03.167, 2004.

Day, K. A., Hibbins, R. E., and Mitchell, N. J.: Aura MLS observations of the westward-propagating s=1, 16-day planetary wave in the stratosphere, mesosphere and lower thermosphere, Atmos. Chem. Phys., 11, 4149–4161, doi:10.5194/acp-11-4149-2011, 2011.

Day, K. A., Taylor, M. J., and Mitchell, N. J.: Mean winds, temperatures and the 16- and 5-day planetary waves in the mesosphere and lower thermosphere over Bear Lake Observatory (42° N, 111° W), Atmos. Chem. Phys., 12, 1571–1585, doi:10.5194/acp-12-1571-2012, 2012.

Dee, D. P., Uppala, S. M., Simmons, A. J., Berrisford, P., Poli, P., Kobayashi, S., Andrae, U., Balmaseda, M. A., Balsamo, G., Bauer, P., Bechtold, P., Beljaars, A. C. M., van de Berg, L., Bidlot, J.,

Bormann, N., Delsol, C., Dragani, R., Fuentes, M., Geer, A. J., Haimberger, L., Healy, S. B., Hersbach, H., Hólm, E. V., Isaksen, L., Kållberg, P., Köhler, M., Matricardi, M., McNally, A. P., Monge-Sanz, B. M., Morcrette, J.-J., Park, B.-K., Peubey, C., de Rosnay, P., Tavolato, C., Thépaut, J.-N., and Vitart, F.: The ERA-Interim reanalysis: configuration and performance of the data assimilation system, Q. J. Roy. Meteor. Soc., 137, 553–597, doi:10.1002/qj.828, 2011.

Dragani, R. and McNally, A. P.: Operational assimilation of ozone-sensitive infrared radiances at ECMWF, Q. J. R. Meteorol. Soc., 139, 2068–2080, doi:10.1002/qj.2106, 2013.

ECMWF: available at: http://www.ecmwf.int/en/forecasts/documentation-and-support/changes-ecmwf-model, last access: 15 June 2015.

ECMWF: https://software.ecmwf.int/wiki/display/IFS/Official+IFS+Documentation, accessed 15 Feb 2016, 2016.

Engelen, R. J. and Bauer, P.: The use of variable CO_2 in the data assimilation of AIRS and IASI radiances, Q. J. R. Meteorol. Soc., 140, 958–965, doi:10.1002/qj.919, 2014.

Eriksson, P., Jimenez, C., and Buehler, S.: Qpack, a general tool for instrument simulation and retrieval work, J. Quant. Spectrosc. Ra., 91, 47–64, doi:10.1016/j.jqsrt.2004.05.050, 2005.

Eriksson, P., Buehler, S., Davis, C., Emde, C., and Lemke, O.: ARTS, the atmospheric radiative transfer simulator, version 2, J. Quant. Spectrosc. Ra., 112, 1551–1558, doi:10.1016/j.jqsrt.2011.03.001, 2011.

Fedulina, I. N., Pogoreltsev, A. I., and Vaughan, G.: Seasonal, interannual and short-term variability of planetary waves in Met Office stratospheric assimilated fields, Q. J. R. Meteorol. Soc., 130, 2445–2458, doi:10.1256/qj.02.200, 2004.

Guharay, A., Batista, P., Clemesha, B., and Buriti, R.: Observations of the intraseasonal oscillations over two Brazilian low latitude stations: a comparative study , J. Atmos. Sol.-Terr. Phy., 120, 62–69, doi:10.1016/j.jastp.2014.08.016, 2014.

Hardiman, S. C., Butchart, N., Charlton-Perez, A. J., Shaw, T. A., Akiyoshi, H., Baumgaertner, A., Bekki, S., Braesicke, P., Chipperfield, M., Dameris, M., Garcia, R. R., Michou, M., Pawson, S., Rozanov, E., and Shibata, K.: Improved predictability of the troposphere using stratospheric final warmings, J. Geophys. Res.-Atmos., 116, D18113, doi:10.1029/2011JD015914, 2011.

Harris, F. J.: On the use of windows for harmonic analysis with the discrete Fourier transform, P. IEEE, 66, 51–83, doi:10.1109/PROC.1978.10837, 1978.

Hildebrand, J., Baumgarten, G., Fiedler, J., Hoppe, U.-P., Kaifler, B., Lübken, F.-J., and Williams, B. P.: Combined wind measurements by two different lidar instruments in the Arctic middle atmosphere, Atmos. Meas. Tech., 5, 2433–2445, doi:10.5194/amt-5-2433-2012, 2012.

Hirooka, T. and Hirota, I.: Normal Mode Rossby Waves Observed in the Upper Stratosphere. Part II: Second Antisymmetric and Symmetric Modes of Zonal Wavenumbers 1 and 2, J. Atmos. Sci., 42, 536–548, doi:10.1175/1520-0469(1985)042<0536:NMRWOI>2.0.CO;2, 1985.

Hirota, I. and Hirooka, T.: Normal Mode Rossby Waves Observed in the Upper Stratosphere. Part I: First Symmetric Modes of Zonal Wavenumbers 1 and 2, J. Atmos. Sci., 41, 1253–1267, doi:10.1175/1520-0469(1984)041<1253:NMRWOI>2.0.CO;2, 1984.

Hocke, K.: Phase estimation with the Lomb–Scargle periodogram method, Ann. Geophys., 16, 356–358, 1998.

Hocke, K., Studer, S., Martius, O., Scheiben, D., and Kämpfer, N.: A 20-day period standing oscillation in the northern winter stratosphere, Ann. Geophys., 31, 755–764, doi:10.5194/angeo-31-755-2013, 2013.

Huang, K. M., Liu, A. Z., Zhang, S. D., Yi, F., Huang, C. M., Gan, Q., Gong, Y., Zhang, Y. H., and Wang, R.: Observational evidence of quasi-27-day oscillation propagating from the lower atmosphere to the mesosphere over 20° N, Ann. Geophys., 33, 1321–1330, doi:10.5194/angeo-33-1321-2015, 2015.

Keckhut, P.: Mid-latitude summer response of the middle atmosphere to short-term solar UV changes, Ann. Geophys., 13, 641–647, doi:10.1007/s00585-995-0641-7, 1995.

Koshyk, J. N., Boville, B. A., Hamilton, K., Manzini, E., and Shibata, K.: Kinetic energy spectrum of horizontal motions in middle-atmosphere models, J. Geophys. Res.-Atmos., 104, 27177–27190, doi:10.1029/1999JD900814, 1999.

Le Pichon, A., Assink, J. D., Heinrich, P., Blanc, E., Charlton-Perez, A., Lee, C. F., Keckhut, P., Hauchecorne, A., Rüfenacht, R., Kämpfer, N., Drob, D. P., Smets, P. S. M., Evers, L. G., Ceranna, L., Pilger, C., Ross, O., and Claud, C.: Comparison of co-located independent ground-based middle-atmospheric wind and temperature measurements with numerical weather prediction models, J. Geophys. Res.-Atmos., 120, 8318–8331, doi:10.1002/2015JD023273, 2015.

Lomb, N. R.: Least-squares frequency analysis of unequally spaced data, Astrophys. Space Sci., 39, 447–462, doi:10.1007/BF00648343, 1976.

Luo, Y., Manson, A. H., Meek, C. E., Thayaparan, T., MacDougall, J., and Hocking, W. K.: Extra long period (20–40 day) oscillations in the mesospheric and lower thermospheric winds: observations in Canada, Europe and Japan, and considerations of possible solar influences, J. Atmos. Sol.-Terr. Phy., 63, 835–852, doi:10.1016/S1364-6826(00)00206-6, 2001.

Luo, Y., Manson, A. H., Meek, C. E., Thayaparan, T., MacDougall, J., and Hocking, W. K.: The 16-day wave in the mesosphere and lower thermosphere: simultaneous observations at Saskatoon

(52° N, 107° W) and London (43° N, 81° W), Canada, J. Atmos. Sol.-Terr. Phy., 64, 1287–1307, doi:10.1016/S1364-6826(02)00042-1, 2002.

McIntyre, M. E. and Palmer, T. N.: Breaking planetary waves in the stratosphere, Nature, 305, 593–600, doi:10.1038/305593a0, 1983.

Müllemann, A. and Lübken, F.-J.: Horizontal winds in the mesosphere at high latitudes, coupling processes in the MLT region, Adv. Space Res., 35, 1890–1894, doi:10.1016/j.asr.2004.11.014, 2005.

National Research Council: United States Space Science Program: Report to COSPAR, Ninth Meeting, National Academy of Sciences, 1966.

Orr, A., Bechtold, P., Scinocca, J., Ern, M., and Janiskova, M.: Improved middle atmosphere climate and forecasts in the ECMWF model through a nonorographic gravity wave drag parameterization, J. Climate, 23, 5905–5926, doi:10.1175/2010JCLI3490.1, 2010.

Press, W. H., Teukolsky, S. A., Vetterling, W. T., and Flannery, B. P.: Numerical Recipes in Fortran 77: The Art of Scientific Computing, 2nd edn., Cambridge University Press, New York, NY, USA, 2001.

Rienecker, M. M., Suarez, M. J., Gelaro, R., Todling, R., Bacmeister, J., Liu, E., Bosilovich, M. G., Schubert, S. D., Takacs, L., Kim, G.-K., Bloom, S., Chen, J., Collins, D., Conaty, A., da Silva, A., Gu, W., Joiner, J., Koster, R. D., Lucchesi, R., Molod, A., Owens, T., Pawson, S., Pegion, P., Redder, C. R., Reichle, R., Robertson, F. R., Ruddick, A. G., Sienkiewicz, M., and Woollen, J.: MERRA: NASA's Modern-Era Retrospective Analysis for Research and Applications, J. Climate, 24, 3624–3648, doi:10.1175/JCLI-D-11-00015.1, 2011.

Rodgers, C. D.: Inverse Methods for Atmospheric Sounding: Theory and Practice, Vol. 2 of Series on Atmospheric, Oceanic and Planetary Physics, World Scientific, Singapore, reprint 2008, 2000.

Rüfenacht, R., Kämpfer, N., and Murk, A.: First middle-atmospheric zonal wind profile measurements with a new ground-based microwave Doppler-spectro-radiometer, Atmos. Meas. Tech., 5, 2647–2659, doi:10.5194/amt-5-2647-2012, 2012.

Rüfenacht, R., Murk, A., Kämpfer, N., Eriksson, P., and Buehler, S. A.: Middle-atmospheric zonal and meridional wind profiles from polar, tropical and midlatitudes with the ground-based microwave Doppler wind radiometer WIRA, Atmos. Meas. Tech., 7, 4491–4505, doi:10.5194/amt-7-4491-2014, 2014.

Salby, M. L.: Rossby normal modes in nonuniform background configurations. Part I: Simple fields, J. Atmos. Sci., 38, 1803–1826, doi:10.1175/1520-0469(1981)038<1803:RNMINB>2.0.CO;2, 1981a.

Salby, M. L.: Rossby normal modes in nonuniform background configurations. Part II. Equinox and solstice conditions, J. Atmos. Sci., 38, 1827–1840, doi:10.1175/1520-0469(1981)038<1827:RNMINB>2.0.CO;2, 1981b.

Scargle, J. D.: Studies in astronomical time-series analysis. II. Statistical aspects of spectral-analysis of unevenly spaced data, Astrophys, J., 263, 835–853, doi:10.1086/160554, 1982.

Scheiben, D., Tschanz, B., Hocke, K., Kämpfer, N., Ka, S., and Oh, J. J.: The quasi 16-day wave in mesospheric water vapor during boreal winter 2011/2012, Atmos. Chem. Phys., 14, 6511–6522, doi:10.5194/acp-14-6511-2014, 2014.

Shepherd, T. G., Koshyk, J. N., and Ngan, K.: On the nature of large-scale mixing in the stratosphere and mesosphere, J. Geophys. Res.-Atmos., 105, 12433–12446, doi:10.1029/2000JD900133, 2000.

Sigmond, M., Scinocca, J. F., Kharin, V. V., and Shepherd, T. G.: Enhanced seasonal forecast skill following stratospheric sudden warmings, Nat. Geosci., 6, 98–102, doi:10.1038/NGEO1698, 2013.

Studer, S., Hocke, K., and Kämpfer, N.: Intraseasonal oscillations of stratospheric ozone above Switzerland, J. Atmos. Sol.-Terr. Phy., 74, 189–198, doi:10.1016/j.jastp.2011.10.020, 2012.

Williams, C. R. and Avery, S. K.: Analysis of long-period waves using the mesosphere-stratosphere-troposphere radar at Poker Flat, Alaska, J. Geophys. Res.-Atmos., 97, 20 855–20 861, doi:10.1038/305593a0, 1992.

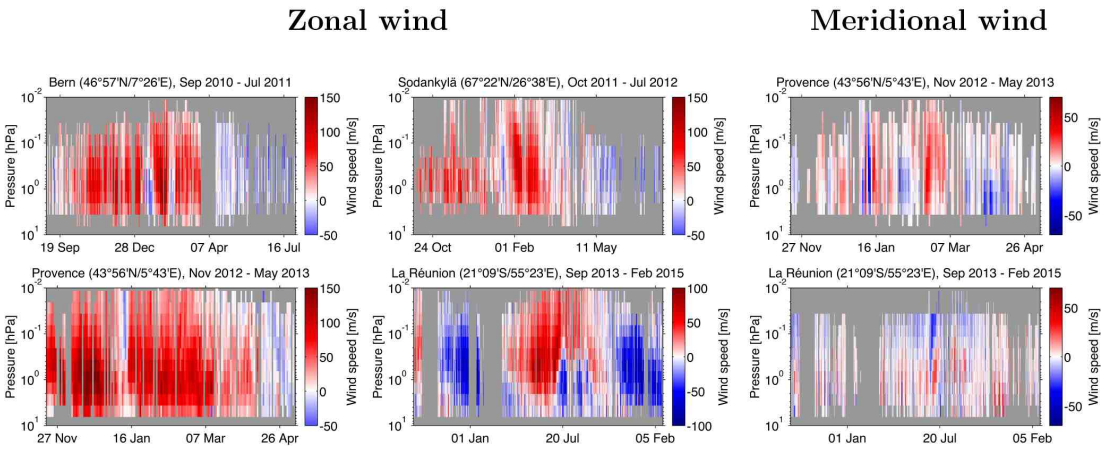

Figure 1. The zonal and meridional wind time series measured by WIRA during four different measurement campaigns analyzed in the present study. The gray areas correspond to data points judged untrustworthy according to the conditions indicated in the text. Please note the different color scale for zonal and meridional wind.

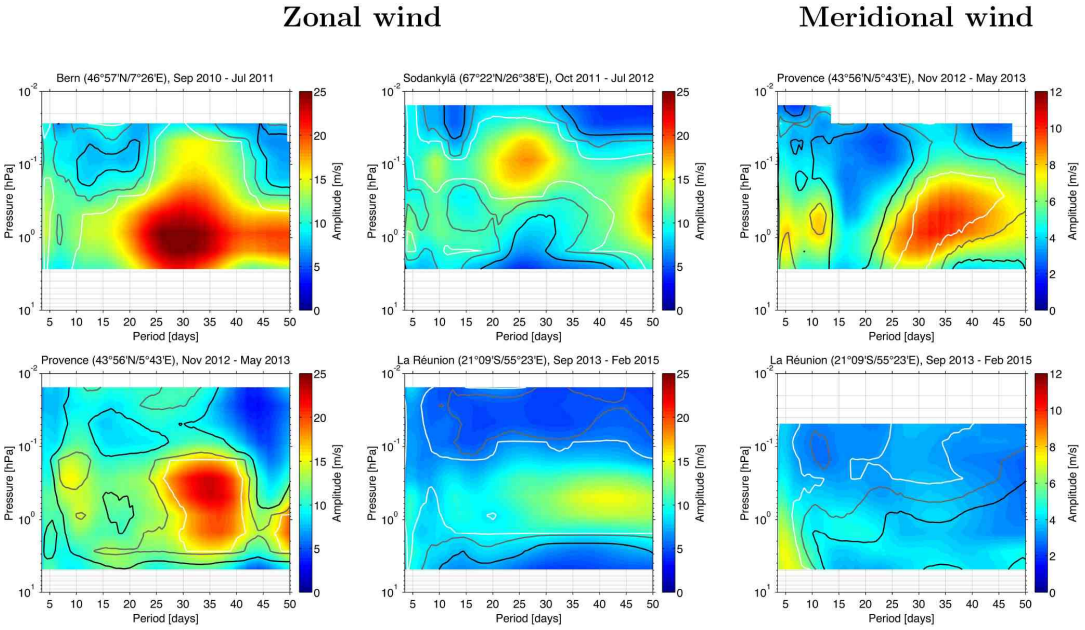

Figure 2. Temporally averaged periodograms of zonal and meridional wind profiles measured by WIRA. The black, gray and white contour lines mark $\alpha = 0.5$, 0.1 and 0.01, where the lowest value, i.e. the white contour, corresponds to the highest significance. The values of α were calculated from Eqs. (5) and (6) based on the average oscillation amplitude and the noise of the entire wind measurement time series determined using the Allan standard deviation (detrended version of the standard deviation e.g. Allan, 1966). The white areas represent altitudes and periods (i.e. window widths) for which the conditions of Eq. (4) are not satisfied, i.e. for which WIRA cannot provide reliable information due to an insufficient number of data points.

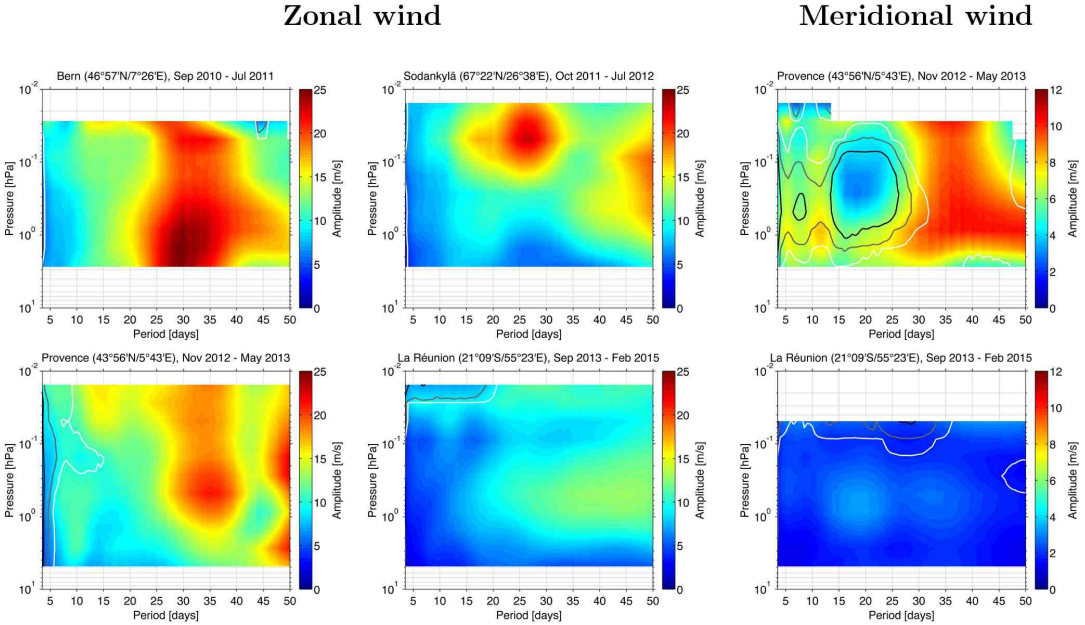

Figure 3. As Fig. 2 but for the scenario ECMWF at WIRA, i.e. for ECMWF profiles convolved with WIRA's averaging kernels and with data gaps introduced where WIRA did not provide reliable measurements.

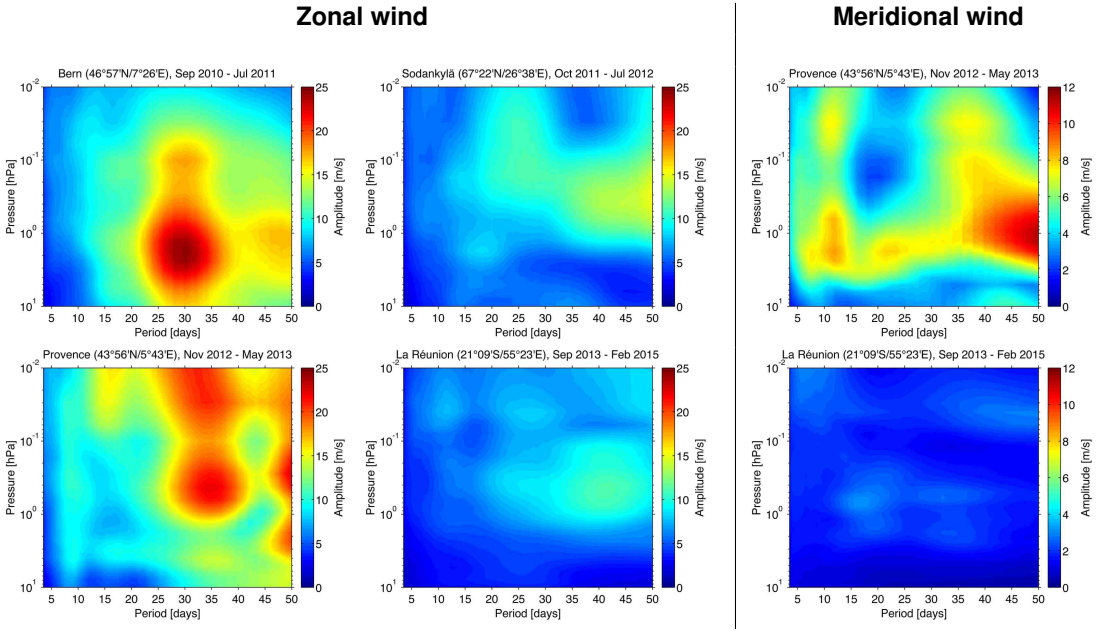

Figure 4. As Fig. 3 but for the unaltered daily average wind data from the ECMWF operational analysis.

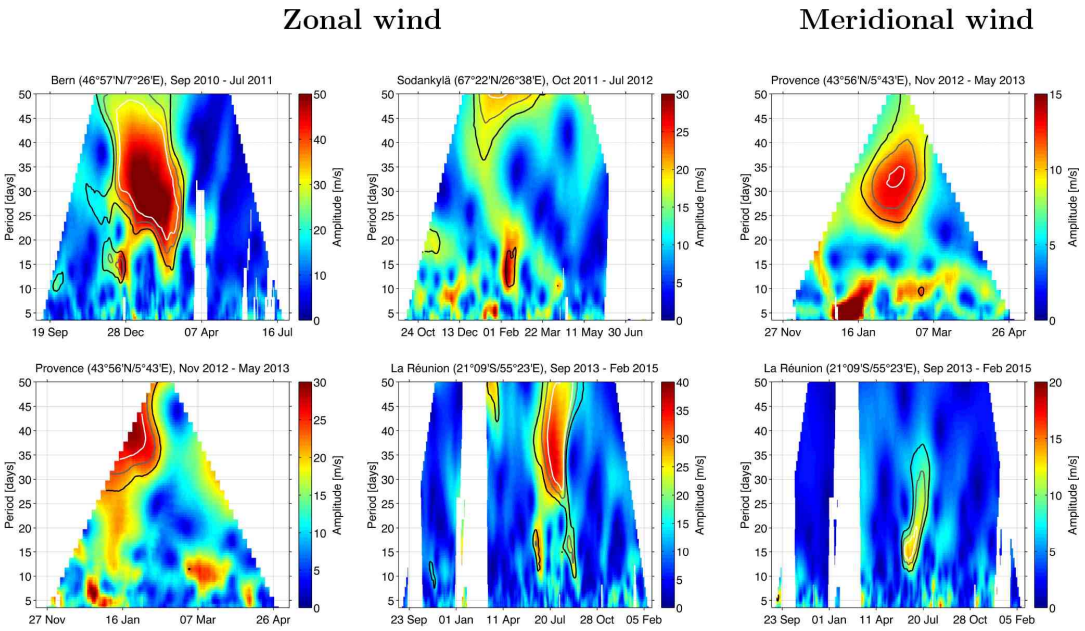

Figure 5. Temporal evolution of the periodogram at stratopause level (0.9 hPa) for wind measurements taken by WIRA. The black, gray and white contour lines mark $\alpha = 0.5$, 0.1 and 0.01 according to Eq. (6). The lowest value, i.e. the white contour, corresponds to highest significance. White areas represent times for which $\mathcal{B}_j$ contains indices before the start date of after the end date of the respective measurement campaign (what entails the trapezoidal shape of the colored area). Other areas are blanked out because the conditions of Eq. (4) are not satisfied, i.e. WIRA cannot provide reliable information due to an insufficient number of data points. Please note the occurrence of 16-day oscillations near the onset and the termination of the extra-long period oscillation in zonal wind for Bern and La Réunion.

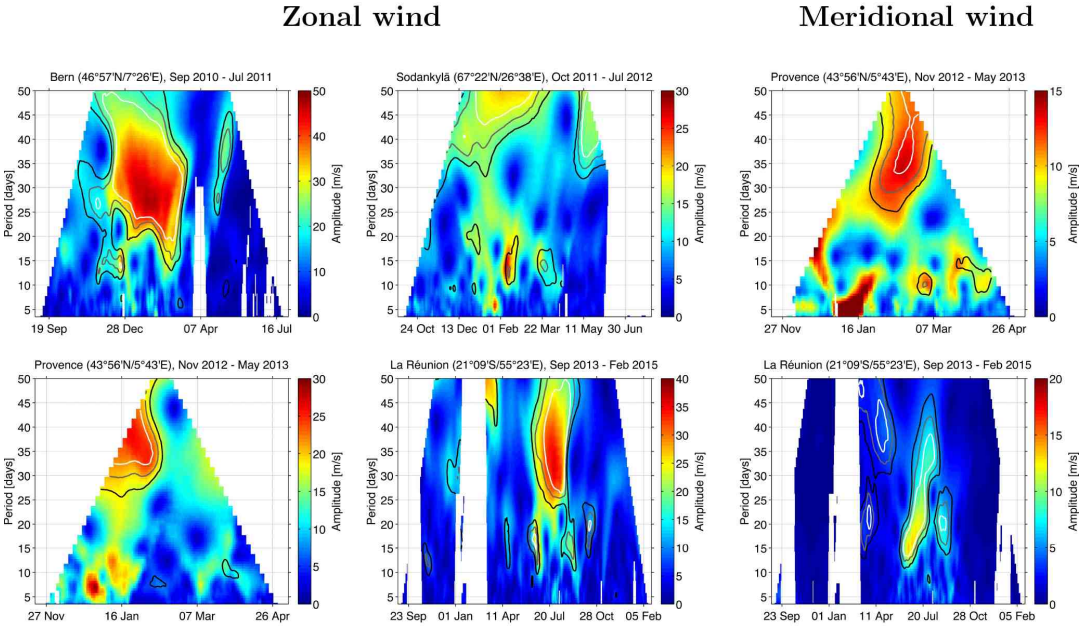

Figure 6. As Fig. 5 but for the scenario ECMWF at WIRA.

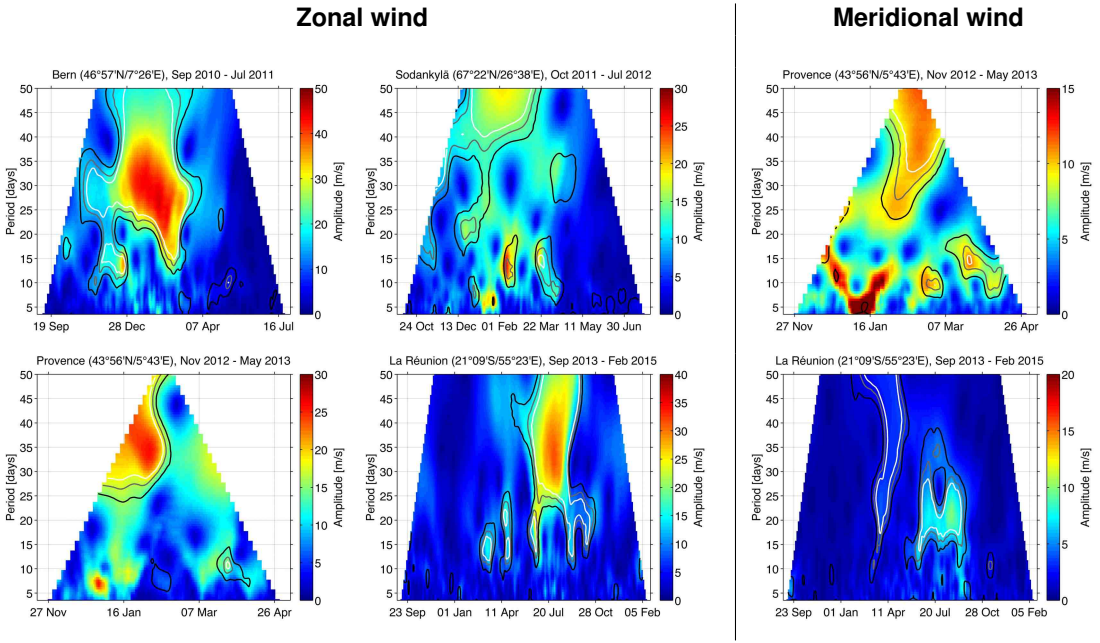

Figure 7. As Fig. 6 but for the unaltered daily average wind data from the ECMWF operational analysis.